Langmuir

Article

pubs.acs.org/Langmuir

# Thermomechanical Transitions of Egg-Ceramide Monolayers

Elisa R. Catapano,[†,‡] M. P. Lillo,[§] C. García Rodríguez,[§] P. Natale,[†,‡] D. Langevin,[∥] F. Monroy,[†,‡] and I. López-Montero*[,†,‡]

[†]Departamento de Química Física I, Universidad Complutense, Ciudad Universitaria s/n, 28040 Madrid, Spain

[‡]Instituto de Investigación Hospital 12 de Octubre (i+12), Avda. de Córdoba s/n, 28041 Madrid, Spain

[§]Grupo de Biofísica Molecular, Instituto Química Física Rocasolano, CSIC, Serrano 119, 28006 Madrid, Spain

[∥]Laboratoire de Physique des Solides, Université Paris-Sud, Rue Nicolas Appert Bâtiment 510, 91405 Orsay, France

**ABSTRACT:** Ceramides have unique biophysical properties. Their high melting temperature and their ability to form lateral domains have converted ceramides into the paradigm of rigid lipids. Here, using shear surface rheology of egg-ceramide Langmuir monolayers, a solid to fluid transition was evidenced as a vanishing shear rigidity at lower temperatures than the lipid melting temperature. Such a mechanical transition, which depends on the lipid lateral pressure, was found in a broad range temperature (40−50 °C). The solid to fluid transition was correlated to a LC to LC+LE phase transition, as confirmed by BAM experiments. Interestingly, together with the softening transition, a supercooling process compatible with a glassy behavior was found upon freezing. A new phase scenario is then depicted that broadens the mechanical behavior of natural ceramides. The phase diversity of ceramides might have important implications in their physiological roles.

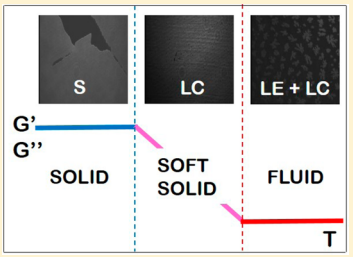




## INTRODUCTION

Ceramides belong to the lipid family of sphingolipids.[1,2] Sphingolipids have attracted great interest in the last years because they are involved in important biological supramolecular structures as lipid domains[3] and more recently identified as active lipids.[4] In particular, ceramides have been claimed to be molecular messengers in cell death or apoptosis,[5] elicited by different stressors such as serum deprivation, irradiation, or heat shock.[6] In mammalian cells, heat shock is produced when temperature rises above 37 °C. In response to heat shock, an increase in the ceramide levels has been reported in different cell types,[6] and the ceramide pool arises from sphingomyelin cleavage by enzymatic conversion.[7] The reason by which heat shock results in raising ceramide levels is still unclear and could stem on the thermotropic properties of ceramides.[2]

Because of their high melting transition temperature (∼90 °C),[8] ceramides are considered to form solid-type layers and are able to modify the physical state of the cell membrane, including membrane fluidity and permeability,[9] lateral domain segregation,[10] and membrane stiffness.[11] Recently, a rich phase behavior has been revealed from compression isotherms studies performed in Langmuir monolayers of palmitoyl ceramide and its mixtures with palmitoyl sphingomyelin.[12,13] For those mixed layers, a variety of liquid phases were found close to physiological temperatures, including liquid-expanded (LE) and liquid-condensed (LC) phases; however, the question about the solid or fluid nature of the different lipid phases attributed to ceramides under thermal change is still waiting for mechanical identification. Strictly speaking, the unequivocal solid character should be determined in mechanical studies of the shear response of monomolecular layers.[14,15] Solids support both compression and shear stresses, while liquids do not resist shear and consequently flow. Here we explore the shear viscoelasticity of egg-ceramide monolayers as a function of temperature and the packing state of the lipid in the Langmuir monolayer. Our results indicate that natural ceramides undergo a solid-to-fluid mechanical transition at lower temperatures than the main bulk melting transition ($T_m \approx 75$ °C). Such a thermal transition occurs from a rigid solid to a fluid state. The transition is followed by a drastic decrease in the shear viscosity of the monolayers.

## EXPERIMENTAL SECTION

**Lipids and Chemicals.** Egg-ceramide was supplied by Avanti Polar Lipids as a powder. Fatty acid composition of egg ceramide was: 1% C14:0, 84.3% C16:0, 5.2% C18:0, 1% C20:0, 1.5% C22:0, 0.7% C24:0, 4.5% C24:1, and 2.8% others.[16] Just before use, the lipids are dissolved in chloroform (Sigma-Aldrich, ≥99.8% purity) to achieve a final concentration of 1 mg/mL. The stock solutions were kept at −20 °C. Experiments on Langmuir monolayers were performed by spreading the lipid on a water subphase. High-purity water was produced by a Milli-Q source system (Millipore, resistivity higher than 18 MΩ cm; surface tension $\gamma$ = 72.6 mN/m at 20 °C).

**Oscillatory Shear Rheology.** We used a shear rheometer (Physica MCR301, Anton Paar) equipped with a biconical bob tool (68.3 mm diameter, 5° cone angle). Temperature control (±0.1 °C) is performed with a Peltier element assisted by an external water thermostat. (See ref 11 for details.) A sinusoidal strain $\gamma$ of amplitude $\gamma_0$ is applied to the monolayer at a frequency $\omega$: $\gamma(t) = \gamma_0 \sin(\omega t)$. In the linear regime, the shear stress is $\sigma(t) = G^*\gamma(t)$, where $G^*$ is the shear viscoelastic modulus $G^* = G' + iG''$, where $G'$ is the storage

**Received:** January 21, 2015
**Revised:** March 5, 2015
**Published:** March 12, 2015

  

DOI: 10.1021/acs.langmuir.5b00229
*Langmuir* 2015, 31, 3912−3918

modulus and $G''$ is the loss modulus, accounting for the dissipation. In this instrument, a given packing state is reached by subsequent dropwise addition of lipid chloroform solution (0.01 mg/mL). The monolayer is left to equilibrate for 1 h and then presheared at a fixed frequency (1 Hz, 0.1% shear amplitude, 1 h, typically) prior to measurements. Despite the high resolution in torque measurements ($\delta\sigma \approx \pm 0.01$ mN/m), the experimental reproducibility is limited by the capacity to reproduce identical monolayer states in different experiments, and the final viscoelastic parameters are affected by a typical experimental error $\sim\delta G'$, $\delta G'' \approx \pm 1$ mN/m. (A detailed discussion is provided in ref 11.)

**Compression Isotherms.** The monolayers were spread from the lipid chloroform solution (1 mg/mL) and the solvent was left to evaporate to record the surface pressure ($\pi$) versus molecular area ($A$) plots. The surface pressure was measured with paper Wilhemy plates. The surface area available to the monolayer is changed by unilateral compression. The surface pressure is measured at the center of the trough using a paper Wilhelmy plate attached to a force sensor (PS4, NIMA). The subphase temperature was controlled by recirculating water from a thermostatic bath (Polyscience) through a fluid circuit placed at the bottom of the trough and measured by a Pt-100 sensor. The experimental setup is placed in a transparent plexiglass box to avoid undesirable air streams or dust deposition on the surface during experiments. We used a Langmuir balance (702BAM, NIMA, U.K.) equipped with two symmetrically moving barriers. The maximum surface area was 700 $cm^2$. In this method, a sole aliquot of 50 $\mu$L of lipid solution was spread onto the free surface of the subphase contained in the Langmuir trough. After chloroform evaporation and monolayer equilibration in the diluted state (1 h after spreading), the compression isotherm was recorded at a constant compression rate of 5 $cm^2$/min. Under these conditions, the strain rates are slow enough ($du/dt \approx 10^{-4}$ $s^{-1}$) to ensure quasi-static compression and near-equilibrium conditions.

**Brewster Angle Microscopy and Ellipsometry.** BAM measurements were performed in a Langmuir balance (702BAM, NIMA, U.K.) installed on a Nanofilm EP3 ellipsometer (Germany) with a polarized incident laser of $\lambda = 532.0$ nm. Ellipsometry was performed at an incidence grazing angle $\theta = 55.2 \pm 0.1°$ to maximize the reflected intensity and the polarization sensibility. The absolute changes of the ellipsometric angles $\delta\Delta = \Delta - \Delta_0$ and $\delta\phi = \phi - \phi_0$ are obtained with respect to the values corresponding to the bare interface (denoted by the subscript 0). The small changes observed in the phase angle ($\delta\phi \approx 0$) are related to the refractive index of the monolayer, $n$. For transparent layers, the relevant information is included in $\delta\Delta$, the only parameter measurable with accuracy.[17] The layer thickness $h$ is proportional to the absolute change in ellipticity $\delta\Delta$. For an optically isotropic layer ($h \ll \lambda$), within the Drude approximation,[17] the linear relationship between ellipticity and film thickness reads

$$\delta\Delta = 4\pi(h/\lambda)(n_w^2 \cos\theta \tan^2\theta)(n_a^2 \tan^2\theta - n_w^2)^{-1}$$
$$(n_w^2 - n_a^2)^{-1}(n_a^2 + n_w^2 - n^2 - (n_a^2 n_w^2/n^2))$$

where $n_a \approx 1.00$ and $n_w \approx 1.33$ are the refractive indices of air and water, respectively, and $n$ is refractive index of the layer ($n \approx 1.49$).[18]

**Differential Scanning Calorimetry.** Hydrated ceramide samples were prepared pipetting the appropriate volume of ceramide solution into a preweighted stainless-steel pan. The organic solvent was removed under vacuum and hydrated to a final concentration of 3 mg/mL. DSC measurements were performed in a MicroCal VP-DSC (Northampton, MA) differential scanning calorimeter at heating/cooling rates of 0.5 °C/min.

## RESULTS AND DISCUSSION

**Shear Viscoelasticity.** The solid character of 2-D monolayers was measured in mechanical experiments probing the shear response of Langmuir monolayers of egg-ceramide. Recently, we have shown the solid character of egg-ceramides monolayers at physiological temperature (37 °C).[11,14,15] Here we revisit the question and we measure the temperature dependence of the shear response. Figure 1 shows the measured values of the storage ($G'$) and loss ($G''$) moduli as

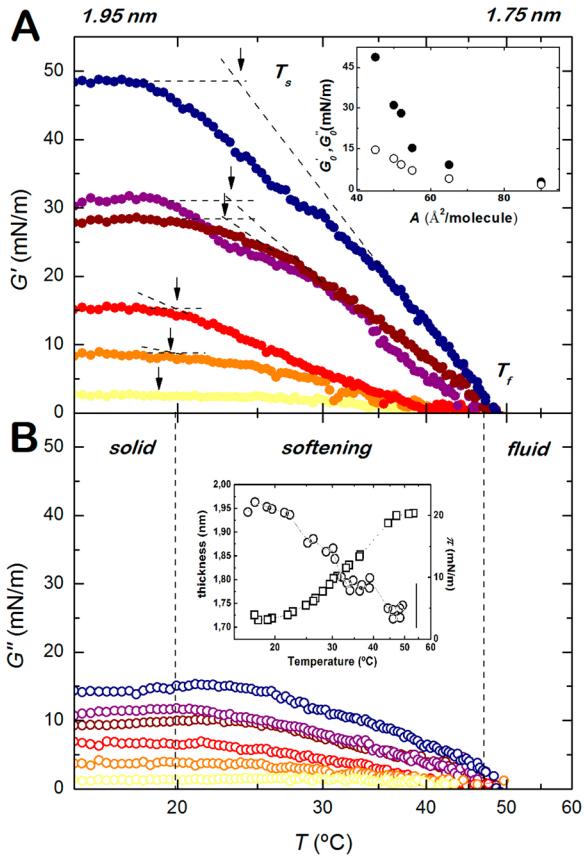


**Figure 1.** Temperature dependence of the shear moduli as obtained from oscillatory shear experiments with $\gamma = 5 \times 10^{-4}$ (0.05%) and performed at different constant surface packing ($A$ = 90 (yellow ●), 65 (orange ●), 55 (red ●), 52 (dark red ●), 50 (purple ●), and 45 Å²/molecule (blue ●)). (A) Storage modulus, $G'$; (B) loss modulus, $G''$. Inset A: $G'_0$ and $G''_0$ plateaux values obtained from ($A$) as a function of the constant lipid surface area. Inset B: Film thickness (circles) and lateral pressure (squares) of egg-ceramides as a function of temperature derived from gray level intensity, as determined by BAM at isocoric conditions. The bar represents the measurement uncertainty for the monolayer thickness.

a function of temperature upon heating runs at different surface concentrations. At low temperatures, the value of the shear modulus is found to be finite and higher than the viscous losses ($G' > G'' > 0$), meaning that the monolayers behave solid-like. Up to a softening temperature $T_s \approx 20$–25 °C, the two moduli remain nearly constant, defining a plateau value, $G'_0$ and $G''_0$, which increases with the lipid surface concentration. (See the inset in Figure 1A.) This feature is a clear distinctive of the solid state of these monolayers. Heating above $T_s$ causes the solid to progressively soften into an intermediate state, where both moduli remain still nonzero but decrease nearly linear with temperature down to a fluidification temperature, $T_f$, at which $G'$ vanishes. Above $T_f$, the ceramide monolayers become liquid ($G' = 0$, $G'' \approx 0$).

The shear data evidence the existence of three different phases in the studied temperature range: a solid (S) phase up to ~20 °C, a thermally soften solid (soft-S) phase from 20 °C up to $T_f$ (40–50 °C), and a fluid (F) phase above $T_f$. To get further structural insight, we determined the ellipsometric


DOI: 10.1021/acs.langmuir.5b00229
Langmuir 2015, 31, 3912–3918

thickness under isochoric conditions along a heating pathway. (See the inset in Figure 1B.) In the solid state, the thickness of egg-ceramides monolayers was 1.95 nm, a value compatible with recent ellipsometric measurements of synthetic ceramides.[19] The softening transition was accompanied by a progressive decrease in the thickness of the monolayer, reaching a minimal value of 1.75 nm when the fluid phase is entered. This thinning (~0.20 nm) is significant and consistent with a change of the tilt of the lipid tails. The thickness is continuous over the transition and continuously decreases with increasing surface pressure, reaching a minimal value in the fluid phase.[20] (See the inset in Figure 1B.)

To get insight, fluid monolayers (52 Å$^2$/molecule) were frozen upon cooling runs initially into the thermoresponsive features of egg-ceramides. In these experiments, the shear modulus rise from zero at high temperatures ($G' = 0$ at $T > 60$ °C) up to finite values at a solidification temperature of ~52 °C. Both $G'$ and $G''$ raised upon cooling to ~45 °C. Then, $G'$ and $G''$ recovered a plateau regime, which is found, however, at values significantly smaller that when the monolayer is initially prepared in the frozen state, suggesting the presence of supercooling effects in the monomolecular films. When experiments were repeated at different cooling rates, smaller plateau values of $G'$ and $G''$ were detected with increasing the temperature ramp rate, a fact pointing to the existence of metastable supercooled states during the solidification process. (See Figure 2A.) The underlying mechanism for the ceramide supercooling could be probably related to nucleation effects, described by a competition between the nucleation and cooling rates. Indeed, condensation into a solid phase requires surpassing an energetic barrier, which should be sufficient to retain the cooled system with the characteristics of the softened states found at higher temperatures. As shown in Figure 2B, LC-lipid domains coexist with a continuous fluid phase at high temperature and high surface packing ($T = 60°$ and 50 Å$^2$/molecule, respectively). Upon cooling, lipid domains grow, forming larger lipid patches of the LC phase. Finally, shiny spots start to appear between the ceramide patches and grow into star-shaped structures that prevented the formation of a continuous condensed phase. A similar softening behavior was observed for the loss shear modulus, which reached values as low as 2 mN/m when the experiment was performed at the maximum cooling rate. (See the inset of Figure 2A.)

**Egg-Ceramide Phase Diagram.** To identify the thermodynamic nature of the three mechanical states and assign them with well-established lipid phases, the pressure−temperature ($\pi-T$) phase diagram for egg-ceramides was explored. As a reference, we used the detailed phase diagram that has been recently reported for synthetic palmitoyl ceramide in Langmuir monolayers.[13] Here, by combining Brewster angle microscopy (BAM) with simultaneous recordings of compression isotherms and isobars, a similar $\pi-T$ phase diagram was constructed for egg-ceramide monolayers. Figure 3 shows the experimental surface pressure−area isotherms of egg-ceramide monolayers at different temperatures. Below 37 °C, no phase transitions were detected as slope kinks along the compression pathway.[15] For molecular areas above 75 Å$^2$, $\pi \approx 0$ and upon further compression abruptly increases up to the collapse. The isotherms are nearly athermal and of the condensed-type, characterized by similar mean molecular area, $A_0$ ($\pi > 0$) = 50−55 Å$^2$. At higher temperatures ($T > 37$ °C), a different behavior is observed. The isotherms become expanded and a change in slope is detected at pressures close to ~30 mN/m. At 52 °C, an

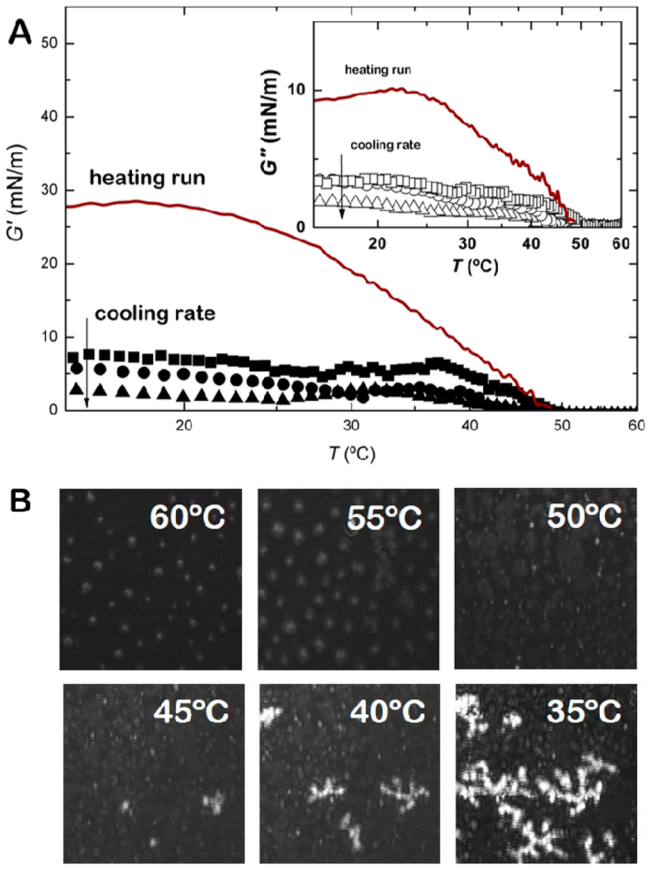


**Figure 2.** Temperature dependence of the shear moduli (obtained at constant surface packing of 50 Å$^2$/molecule) as obtained from oscillatory shear experiments upon different cooling rates $\nu = 0.25$ (■), 0.375 (●), and 0.75 (▲) °C/min. (A) Storage modulus, $G'$; (inset) loss modulus, $G''$. The solid line represents $G'(T)$ and $G''(T)$ as obtained upon heating for an egg-ceramide monolayer with similar lipid surface packing. (B) Surface texture of egg-ceramide condensation upon a cooling sweep as revealed by BAM.

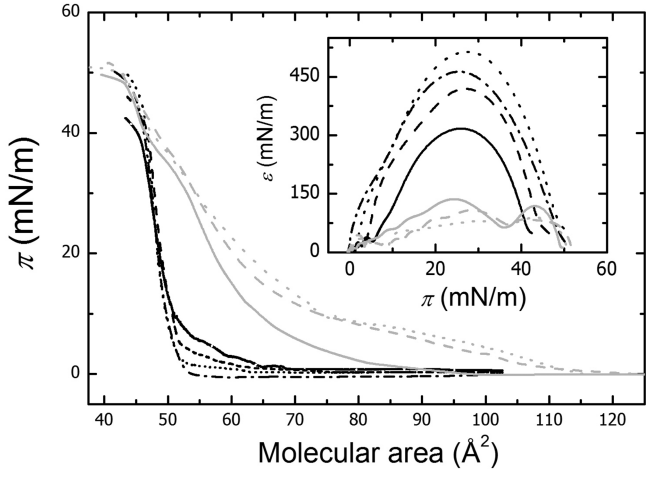


**Figure 3.** Surface pressure $\pi-A$ isotherms of egg-ceramide monolayers measured upon uniaxial and at different temperatures: gray dotted line, 52 °C; gray dashed line, 48 °C; gray solid line, 44 °C; black dashed−dotted line, 37 °C; black dotted line, 30 °C; black dashed line, 20 °C; and black solid line, 10 °C. (Inset) Elastic compression moduli of the egg-ceramide monolayers calculated as the numerical derivative of the experimental $\pi-A$ isotherms; this is $\varepsilon = -((\partial\Pi)/(\partial A))A$.



DOI: 10.1021/acs.langmuir.5b00229
*Langmuir* 2015, 31, 3912−3918

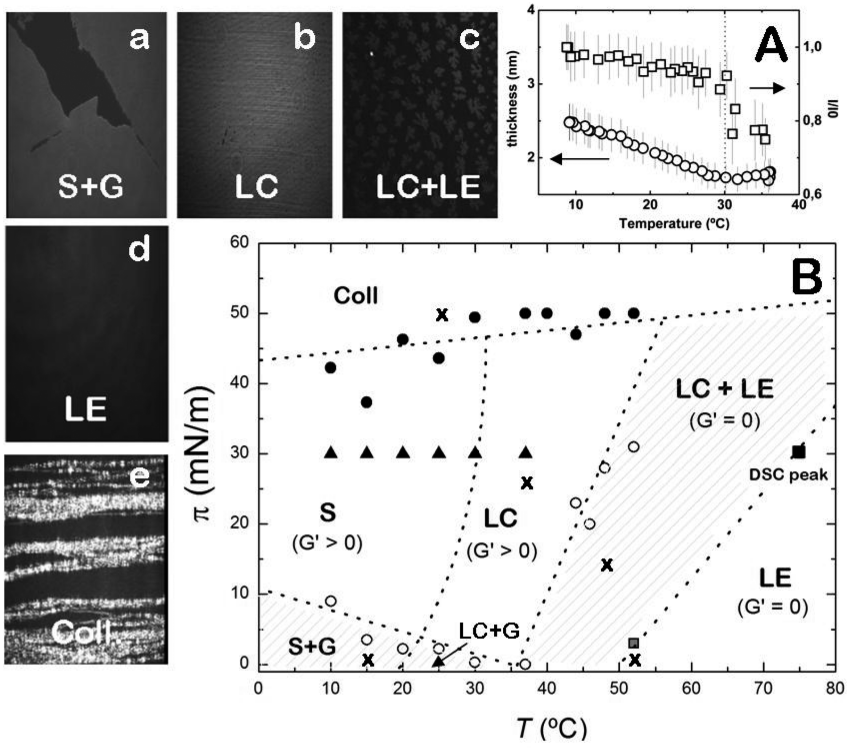


**Figure 4.** (a–e) BAM micrographs representative of different egg-ceramide monolayer states (S, solid; G, gas; LC, liquid-condensed; LE, liquid-expanded; and Coll, collapse). (A) Film thickness (circles) of egg-ceramides as a function of temperature during an isobaric transformation derived from gray level intensity (squares). (B) Surface pressure $\pi$–$T$ phase diagram for egg-ceramide monolayers constructed from isotherms (circles) and isobars (triangles) and from DSC measurements (square). The "x" symbols indicate where the BAM micrographs were taken. The surface pressure in DSC experiments is supposed to be close to 30 mN/m, the biologically relevant pressure in bilayers ($\pi$bil ≈ 30 mN/m). Black symbols correspond to second-order transitions and gray and white symbols correspond to the beginning and the end of first-order transitions, respectively. The gray shadowed areas indicate phase coexistence regions. Each phase is characterized by $G' \geq 0$.

additional change in slope was detected at lower pressures (~5 mN/m). These slope changes might reveal second-order transitions.

To quantitatively characterize the different states, we calculated the uniaxial compression modulus as the numerical derivative of the experimental $\pi$–$A$ isotherms; this is $\varepsilon = -((\partial\Pi)/(\partial A))A$. (See the inset in Figure 3.) Below 37 °C, the compression moduli showed a main maximum at pressures around 25–30 mN/m, the surface state equivalent to the biologically relevant packing.[21] Egg-ceramides exhibited a very low compressibility, with $\varepsilon$ being hundreds of mN/m.[15] Further compression reduces $\varepsilon$, as expected, because of the full compressibility provided by the 3D arrangement of the collapsed monolayer; however, at high temperatures, the elastic moduli decreased to ~100 mN/m, a typical value for fluid phases.[22,23] For the highest temperature, 52 °C, a second maximum was found at 4 mN/m, corresponding to the less close-packed transition found in the isotherm. The absolute value of the secondary maximum was much smaller ($\varepsilon_2 \approx 50$ mN/m) that the one displayed by the main peak. Above $T_f$, egg-ceramides are characterized by a zero shear modulus but a finite compressibility modulus, as usual above a solid to a fluid transition.

Additional information can be obtained from the surface texture of Langmuir monolayers. Figure 4 shows different surface textures representative for different lipid phases previously described. For clarity, we have used the same nomenclature recently used for palmitoyl ceramide.[13,24] At low temperatures and low pressures, a solid + gas (S+G) phase was observed (Figure 4a). The lipid patches were observed to have rectilinear edges, which is typical for solid materials. Upon compression, a homogeneous solid phase was reached by merging the lipid platforms. This S+G to S transition was detected at lower temperatures when compressing at higher pressures. From the solid phase (at 30 mN/m), an increase in temperature produced a decrease in the optical reflectance (Figure 4b), suggesting a S to LC transition at 30 °C. The decrease in reflectance indicates a decrease in film thickness (2.4 to 1.8 nm), supporting the fact that the LC phase may be tilted. (See Figure 4A.) The thickness (and the tilt) remains constant after the phase transition, as expected. This transition (LC to S) should be detected as a kink on isotherms at low temperatures ($15 < T < 37$ °C), with the compressibility decreasing further after the pressure kink. The transition to an untilted phase is probably a second-order transition.[25] Unlike palmitoyl ceramide,[13] egg-ceramide did not display any LC to S transition, probably due to the supercooling effects, i.e., the slow-kinetic character of the phase transition. (See Figure 2.) Because of the heterogeneous composition of egg-ceramides, the so-called solid (untilted) phase could be an amorphous solid. Synchrotron X-ray diffraction experiments could serve to determine the structure at the molecular level of egg-ceramides to unequivocally discriminate their crystalline or amorphous character.[26] In the latter case, ceramides could behave as a glass, and the thermal softening transition observed in Figure 1 could be attributed to a glass transition (instead of a S to LC transition), which occurs at a glass temperature, $T_g$, being identified as the temperature at which the shear modulus starts



DOI: 10.1021/acs.langmuir.5b00229
Langmuir 2015, 31, 3912–3918

to decrease from $G'_0$ down to zero in the fluid state. Glasses can be constituted of polymers,[27] granular materials,[28] or colloidal dispersions.[29] Together with the lack of reversibility during temperature cycles, that is, supercooling effects,[27] the thermomechanical transition shown at low temperature, could be compatible with a 2D glass-like behavior, suggested for the first time here for lipid monolayers.

At temperatures above 37 °C, an LC+LE coexistence was observed as already reported for low lateral pressures $\pi \approx 0.5$ mN/m for other lipid systems.[30] Figure 4c shows a dark continuous phase LE phase decorated by brighter LC domains. Upon compression, the liquid-condensed domains coalesced to form a homogeneous LC phase: the higher the temperature, the higher the transition pressure. This transition coincides with the pressures of the elastic moduli maxima displayed in Figure 3B. Finally, an LE to LE+LC transition was detected at 52 °C and at lateral pressures as low as ∼4 mN/m. The LE phase (Figure 4d) is characterized by a low compressibility modulus of ∼50 mN/m (Figure 3B). Finally, a crumpled surface is observed when ceramide monolayers reached the collapse (Figure 4e). The thicker regions, characterized by a very intense bright, were revealed as surface ruffles that increased their thickness upon further compression. All results are summarized in the pressure−temperature phase diagram obtained for egg-ceramide monolayers and shown in Figure 4B. We were unable to perform compression isotherms and topographical images at temperatures higher than 55 °C because of the rapid evaporation of the subphase and its condensation on the lenses of the BAM.

**DSC Experiments.** DSC experiments were performed then on stacked multilayers to understand the phase behavior of egg-ceramides at higher temperatures[8]. Figure 5 shows representative DSC thermograms (heating and cooling scans) of two different thermotropic transitions of egg-ceramide. DSC heating scan shows a broad endothermic transition centered at ∼75 °C. Interestingly, the main transition is accompanied by one side endothermic peak at lower temperature ($T \approx 45$ °C). The DSC signal was further explored by decomposing the endotherms into individual components to accurately determine the two transition temperatures. We are unable to fit the curve with only two components, and thus the best-fit requires three components centered at 45.7, 67.2, and 74.4 °C ($\Delta H = Cp^*\Delta T = 4$, 24.4, and 14.9 kcal/mol, respectively). The cooling scan (inset, Figure 5) displays both the broad exothermic peak and also the exothermic shoulder at lower temperatures. As in the heating scan, the DSC cooling curve was also decomposed in three exothermic peaks, centered at similar transition temperatures: 44.7, 65.3, and 74.5 °C. These results are compatible with the previously reported thermotropic behavior of C16-(palmitoyl)-ceramide,[8,31] where an endothermic transition at ∼90 °C and a broad exothermic transition at ∼64 °C were observed. From X-ray diffraction experiments, a phase diagram for the multilamellar suspension was depicted in those experiments, that is, a metastable bilayer gel phase that transforms into a thinner (tilted) stable bilayer phase at 64 °C and finally into a fully melted-chain phase at ∼90 °C. It is worth noting that the untilted−tilted phase transition at 64 °C is 40 °C higher than the S to LC transition in palmitoyl ceramide monolayers (20−25 °C).[13]

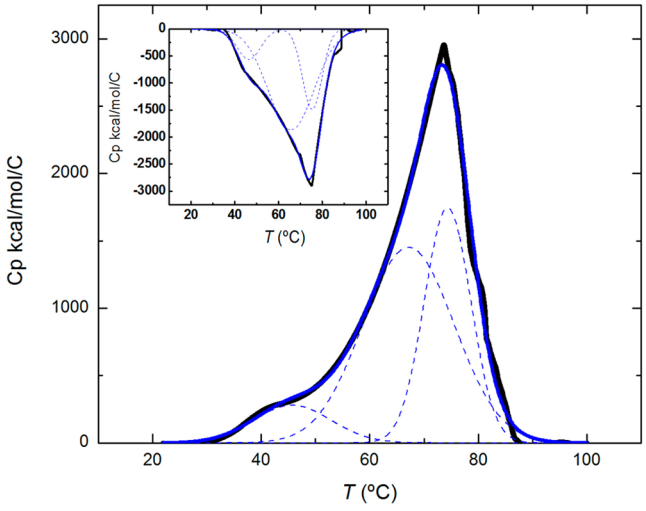


**Figure 5.** DSC thermograms of egg-ceramides upon heating and upon cooling (inset). The main endothermic/exothermic transition was fitted to three Gaussian components (dashed lines).

Our data show that the fully melted-chain phase was shifted to ∼75 °C, probably due to the heterogeneous composition of egg-ceramide[32] and to dimensionality effects. The transition detected at low temperature (∼45 °C) might correspond to the mechanical solid-to-fluid transition and the thermodynamic LC to LC+LE transition; however, the low dimensionality effects, that is the different behavior found in multilayer systems compared with monomolecular monolayers, should also be taken into account, and the peak at ∼45 °C could also correspond to the softening transition (20−25 °C), shifted to higher temperatures because of bulk effects. A well-recognized experimental fact is that polymer films have glass-transition temperatures lower than those of the bulk material.[33] Here ceramide monolayers could display a similar behavior, pointing out the possible existence of a glass transition in lipid Langmuir films.

## CONCLUSIONS

In summary, a new thermomechanical picture can be depicted for egg-ceramides. At very low temperatures (<20−25 °C) ceramides behave as solid materials able to support shear deformations. Above this temperature, ceramides are mechanically softened but still show solid features ($G' > G'' > 0$). At near-above physiological temperature (45 °C for lateral pressure $\pi = 25$ mN/m) the condensed phase enters a LC +LE phase characterized by a vanishing shear moduli but supporting compression deformations, indicative for a macroscopic fluid with microscopic condensed domains coexisting within the LE phase. One could expect that the presence of ordered nuclei within the fluid phase could increase the membrane rigidity under shear or compression; however, the condensed domains are no longer connected but the system can flow through fluid 2D channels made of the continuous LE phase.[34,35] In addition, molecular disorder and lubrication effects might enhance the fluid character of biphasic mixtures.[14] Finally, the monolayer is viscoelastic only in the monophasic LC state, where the condensed domains form a continuous phase. Interestingly, the fluid phase becomes arrested upon cooling, and the phase-transition temperature shifted to lower temperatures. (See Figure 2.) Because the monolayer was prepared at high temperature here, a softening effect produced by the spreading solvent, which could remain trapped in the monolayer, can be discarded. The percolation of LC domains should require an extra energy supply to form the continuous


DOI: 10.1021/acs.langmuir.5b00229
Langmuir 2015, 31, 3912−3918

phase. Although structural information is needed, this scenario is also compatible with a glass transition in egg-ceramide monolayers.

This composite viscoregulated system might have important consequences in thermoregulated biological processes where ceramides are involved as the control of heat shocks, for instance. During heat shock, cells also produce specific subset of proteins called heat shock proteins (HSPs).[36] Furthermore, heat shock results in a rapid increase in cell ceramide levels by a still unclear mechanism.[6] In conjunction with the association of HSPs with phospholipid bilayers,[37] ceramide phase behavior may regulate membrane fluidity and polymorphism to finally preserve membrane integrity during thermal stress. Because a solid-to-fluid transition occurs at temperatures that are close to the heat stress ones, one might hypothesize about the changes in membrane fluidity promoted by the newly formed ceramide. Additionally, supercooling processes may act as a security system to avoid sudden membrane stiffening upon freezing back to physiological temperatures; however, two important facts must be considered. First, the well-known stiffening effect produced by the newly enzymatically generated ceramide on fluid membranes.[38] The apparent counterbalance of the membrane rigidification and the ceramide phase transition shown here must be solved. Second, it has now become clear that some functions of ceramides are chain-length-dependent.[39] However, egg-ceramides used here are mainly composed of C16:0 acyl chains; therefore, further investigation is required to generalize the results presented here to all ceramides within a biological context. These facts may be sound when interpreted as part of the multiple-time-domain ceramide generation activity described for sphingomyelinase in model membranes.[40] The present study provides an important piece of information about the thermomechanical behavior of egg-ceramides that can be relevant for the understanding of their physiological roles.

## AUTHOR INFORMATION

### Corresponding Author

*E-mail: ivanlopez@quim.ucm.es.

### Notes

The authors declare no competing financial interest.

## ACKNOWLEDGMENTS

This work was supported by the ERC Starting Grant "MITOCHON" (ERC-StG-2013-883188) and "Programa Ramon y Cajal" (RYC-2013-12609) from the Spanish Ministry of Economy MINECO (I.L.-M.), the FPU program from MINECO (AP2009-4199) (E.R.C), the project FIS2012-35723 from MINECO (F.M.), S2013/MIT-2807 from the Government of Madrid Area (CAM) (F.M.), and the project CTQ2010-1645/BQU from MINECO (C.G.R., M.P.L.). We thank to Department of Biochemistry and Molecular Biology and to CAI Espectrocopía (Unidad Raman - Infrarrojo-Correlador) of UCM for providing access to DSC and BAM experiments, respectively.

## ABBREVIATIONS:

BAM, Brewster angle microscopy; DSC, differential scanning calorimetry; G, shear modulus; LC, liquid condensed; LE, liquid expanded; $T_f$, fluid temperature; $T_g$, glass temperature; $T_m$, melting temperature; $T_s$, softening temperature; S, solid

## REFERENCES

(1) Slotte, J. P. Biological functions of sphingomyelins. *Prog. Lipid Res.* **2013**, *52*, 424−437.
(2) Goñi, F. M.; Alonso, A. Biophysics of sphingolipids I. Membrane properties of sphingosine, ceramides and other simple sphingolipids. *Biochim. Biophys. Acta, Biomembr.* **2006**, *1758*, 1902−1921.
(3) Simons, K.; Ikonen, E. Functional rafts in cell membranes. *Nature* **1997**, *387*, 569−572.
(4) Contreras, F. X.; Ernst, A. M.; Haberkant, P.; Björkholm, P.; Lindahl, E.; Gonen, B.; Tischer, C.; Elofsson, A.; von Heijne, G.; Thiele, C.; Pepperkok, R.; Wieland, F.; Brügger, B. Molecular recognition of a single sphingolipid species by a protein's transmembrane domain. *Nature* **2012**, *481*, 525−529.
(5) Kolesnick, R.; Hannun, Y. A. Ceramide and apoptosis. *Trends Biochem. Sci.* **1999**, *24*, 224−225.
(6) Chang, Y.; Abe, A.; Shayman, J. A. Ceramide formation during heat shock: A potential mediator of alpha B-Crystallin transcription. *Proc. Natl. Acad. Sci. U.S.A.* **1995**, *92*, 12275−12279.
(7) Bartke, N.; Hannun, Y. A. Bioactive sphingolipids: metabolism and function. *J. Lipid Res.* **2009**, *50*, S91−S96.
(8) Shah, J.; Atienza, J. M.; Rawlings, A. V.; Shipley, G. G. Physical-Properties of Ceramides - Effect of Fatty-Acid Hydroxylation. *J. Lipid Res.* **1995**, *36*, 1945−1955.
(9) López-Montero, I.; Monroy, F.; Vélez, M.; Devaux, P. F. Ceramide: From lateral segregation to mechanical stress. *Biochim. Biophys. Acta, Biomembr.* **2010**, *1798*, 1348−1356.
(10) Pinto, S. N.; Silva, L. C.; Futerman, A. H.; Prieto, M. Effect of ceramide structure on membrane biophysical properties: The role of acyl chain length and unsaturation. *Biochim. Biophys. Acta, Biomembr.* **2011**, *1808*, 2753−2760.
(11) Catapano, E. R.; Arriaga, L. R.; Espinosa, G.; Monroy, F.; Langevin, D.; López-Montero, I. Solid Character of Membrane Ceramides: A Surface Rheology Study of Their Mixtures with Sphingomyelin. *Biophys. J.* **2011**, *101*, 2721−2730.
(12) Busto, J. V.; Fanani, M. L.; De Tullio, L.; Sot, J.; Maggio, B.; Goñi, F. M.; Alonso, A. Coexistence of Immiscible Mixtures of Palmitoylsphingomyelin and Palmitoylceramide in Monolayers and Bilayers. *Biophys. J.* **2009**, *97*, 2717−2726.
(13) Fanani, M. L.; Maggio, B. Phase state and surface topography of palmitoyl-ceramide monolayers. *Chem. Phys. Lipids* **2010**, *163*, 594−600.
(14) Espinosa, G.; López-Montero, I.; Monroy, F.; Langevin, D. Shear rheology of lipid monolayers and insights on membrane fluidity. *Proc. Natl. Acad. Sci. U.S.A.* **2011**, *108*, 6008−6013.
(15) López-Montero, I.; Catapano, E. R.; Espinosa, G.; Arriaga, L. R.; Langevin, D.; Monroy, F. Shear and Compression Rheology of Langmuir Monolayers of Natural Ceramides: Solid Character and Plasticity. *Langmuir* **2013**, *29*, 6634−6644.
(16) Do, U. H.; Ramachandran, S. Mild alkali-stable phospholipids in chicken egg yolks: characterization of 1-alkenyl and l-alkyl-snglycero-3-phosphoethanolamine, sphingomyelin, and 1-alkyl-sn-glycero-3-phosphocholine. *J. Lipid Res.* **1980**, *21*, 888−894.
(17) Azzam, R. M. A.; Bashara, N. M. *Ellipsometry and Polarized Light*; North-Holland: Amsterdam, 1987.
(18) Howland, M. C.; Szmodis, A. W.; Sanii, B.; Parikh, A. N. Characterization of physical properties of supported phospholipid membranes using imaging ellipsometry at optical wavelengths. *Biophys. J.* **2007**, *92*, 1306−1317.
(19) Dupuy, F.; Fanani, M. L.; Maggio, B. Ceramide N-Acyl Chain Length: A Determinant of Bidimensional Transitions, Condensed Domain Morphology, and Interfacial Thickness. *Langmuir* **2011**, *27*, 3783−3791.
(20) Kenn, R. M.; Böhm, C.; Bibo, A. M.; Peterson, I. R.; Möhwald, H.; Alsnielsen, J.; Kjaer, K. Mesophases and Crystalline Phases in Fatty-Acid Monolayers. *J. Phys. Chem.* **1991**, *95*, 2092−2097.
(21) Marsh, D. Lateral pressure in membranes. *Biochim. Biophys. Acta, Rev. Biomembr.* **1996**, *1286*, 183−223.
(22) López-Montero, I.; Arriaga, L. R.; Monroy, F.; Rivas, G.; Tarazona, P.; Vélez, M. High fluidity and soft elasticity of the inner



DOI: 10.1021/acs.langmuir.5b00229
*Langmuir* 2015, 31, 3912−3918

membrane of Escherichia coli revealed by the surface rheology of model Langmuir monolayers. *Langmuir* **2008**, *24*, 4065−4076.
(23) López-Montero, I.; Arriaga, L. R.; Rivas, G.; Vélez, M.; Monroy, F. Lipid domains and mechanical plasticity of Escherichia coli lipid monolayers. *Chem. Phys. Lipids* **2010**, *163*, 56−63.
(24) Harkins, W. D.; Young, T. F.; Boyd, E. The Thermodynamics of Films: Energy and Entropy of Extension and Spreading of Insoluble Monolayers. *J. Chem. Phys.* **1940**, *8*, 954−965.
(25) Albrecht, O.; Gruler, H.; Sackmann, E. Polymorphism of Phospholipid Monolayers. *J. Phys. (Paris)* **1978**, *39*, 301−313.
(26) Kaganer, V. M.; Möhwald, H.; Dutta, P. Structure and phase transitions in Langmuir monolayers. *Rev. Mod. Phys.* **1999**, *71*, 779−819.
(27) Arriaga, L. R.; Monroy, F.; Langevin, D. The polymer glass transition in nanometric films. *Europhys. Lett.* **2012**, *98*, 38007.
(28) Liu, A. J.; Nagel, S. R. Nonlinear dynamics - Jamming is not just cool any more. *Nature* **1998**, *396*, 21−22.
(29) Mattsson, J.; Wyss, H. M.; Fernandez-Nieves, A.; Miyazaki, K.; Hu, Z. B.; Reichman, D. R.; Weitz, D. A. Soft colloids make strong glasses. *Nature* **2009**, *462*, 83−86.
(30) Karttunen, M.; Haataja, M. P.; Saily, M.; Vattulainen, I.; Holopainen, J. M. Lipid Domain Morphologies in Phosphatidylcholine-Ceramide Monolayers. *Langmuir* **2009**, *25*, 4595−4600.
(31) Chen, H. C.; Mendelsohn, R.; Rerek, M. E.; Moore, D. J. Fourier transform infrared spectroscopy and differential scanning calorimetry studies of fatty acid homogeneous ceramide 2. *Biochim. Biophys. Acta, Biomembr.* **2000**, *1468*, 293−303.
(32) Ramstedt, B.; Leppimäki, P.; Axberg, M.; Slotte, J. P. Analysis of natural and synthetic sphingomyelins using high-performance thin-layer chromatography. *Eur. J. Biochem.* **1999**, *266*, 997−1002.
(33) Forrest, J. A.; Jones, R. L. The Glass Transition and Relaxation Dynamics in Thin Polymer Films. In *Polymer Surfaces, Interfaces and Thin Films*; Karim, A., Kumar, S., Eds.; World Scientific Publishing Co. Pte. Ltd.: River Edge, NJ, 2000; p 251.
(34) Arriaga, L. R.; López-Montero, I.; Ignés-Mullol, J.; Monroy, F. Domain-Growth Kinetic Origin of Nonhorizontal Phase Coexistence Plateaux in Langmuir Monolayers: Compression Rigidity of a Raft-Like Lipid Distribution. *J. Phys. Chem. B* **2010**, *114*, 4509−4520.
(35) Caruso, B.; Mangiarotti, A.; Wilke, N. Stiffness of Lipid Monolayers with Phase Coexistence. *Langmuir* **2013**, *29*, 10807−10816.
(36) Lindquist, S.; Craig, E. A. The Heat-Shock Proteins. *Annu. Rev. Genet.* **1988**, *22*, 631−677.
(37) Tsvetkova, N. M.; Horvath, I.; Torok, Z.; Wolkers, W. F.; Balogi, Z.; Shigapova, N.; Crowe, L. M.; Tablin, F.; Vierling, E.; Crowe, J. H.; Vigh, L. Small heat-shock proteins regulate membrane lipid polymorphism. *Proc. Natl. Acad. Sci. U.S.A.* **2002**, *99*, 13504−13509.
(38) Härtel, S.; Fanani, M. L.; Maggio, B. Shape transitions and lattice structuring of ceramide-enriched domains generated by sphingomyelinase in lipid monolayers. *Biophys. J.* **2005**, *88*, 287−304.
(39) Grosch, S.; Schiffmann, S.; Geisslinger, G. Chain length-specific properties of ceramides. *Prog. Lipid Res.* **2012**, *51*, 50−62.
(40) Chao, L.; Gast, A. P.; Hatton, T. A.; Klays, F. J. Sphingomyelinase-Induced Phase Transformations: Causing Morphology Switches and Multiple-Time-Domain Ceramide Generation in Model Raft Membranes. *Langmuir* **2010**, *26*, 344−356.



DOI: 10.1021/acs.langmuir.5b00229
*Langmuir* 2015, 31, 3912−3918